



**HAL**  
open science

## Imperfect interfaces with XFEM: new developments in enrichment function

Q.-Z. Zhu, Julien Yvonnet, J. F. Shao, Qi-Chang He

► **To cite this version:**

Q.-Z. Zhu, Julien Yvonnet, J. F. Shao, Qi-Chang He. Imperfect interfaces with XFEM: new developments in enrichment function. ECCOMAS Thematic Conference on the Extended Finite Element Method - Partition of unity enrichment: Recent Developments and Applications, Jun 2011, United Kingdom. <hal-00749196>

**HAL Id: hal-00749196**

**<https://hal.science/hal-00749196v1>**

Submitted on 7 Nov 2012

HAL is a multi-disciplinary open access archive for the deposit and dissemination of scientific research documents, whether they are published or not. The documents may come from teaching and research institutions in France or abroad, or from public or private research centers.

L'archive ouverte pluridisciplinaire HAL, est destinée au dépôt et à la diffusion de documents scientifiques de niveau recherche, publiés ou non, émanant des établissements d'enseignement et de recherche français ou étrangers, des laboratoires publics ou privés.



HAL Authorization

# Imperfect interfaces with XFEM: new developments in enrichment function

Q.Z. Zhu<sup>1</sup>, J. Yvonnet<sup>1</sup>, J.F. Shao<sup>2</sup>, Q.C. He<sup>1</sup>

<sup>1</sup> Université Paris-Est, France, {qizhi.zhu,j.yvonnet,qi-chang.he}@univ-paris-est.fr

<sup>2</sup> Université Lille 1, France, jianfu.shao@univ-lille1.fr

## 1 Introduction

Discontinuous problems with imperfect interfaces are often encountered in mechanics and engineering science, and their influences on the mechanical behavior of materials and structures has long been recognized. Among all the imperfect interface models in elastostatic context, the spring-layer interface model and the coherent interface model are the two most widely used ones. Initially provoked from phenomenological reasons, these two interface models have been derived by using asymptotic methods through an equivalent replacement of the three-phase configuration by a two-phase configuration (Figure 1). However, analytical results available are still limited to some very simple cases.

In the context of the extend finite element method (XFEM) [1][2], numerical techniques have been developed for modelling imperfect interfaces with complex geometries [3][4]. The present work is devoted to further studies on this topic. For each of the aforementioned interface models, the weak form of the initial problem and an appropriate enrichment function are delivered. Particularly, a unified material-dependent formulation linking two specific functions is proposed. Moreover, a simple numerical application to spring-layer imperfect interface problem is presented.

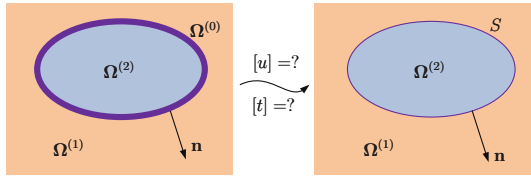


Figure 1: Equivalent replacement of the perfectly bonded three-phase configuration by a two-phase configuration involving imperfect interface  $\mathcal{S}$

## 2 Problem statement

Let  $\Omega^{(1)}$  and  $\Omega^{(2)}$  be two adjoining bulk phase in a solid, as shown in Figure 1(right). The interface between  $\Omega^{(1)}$  and  $\Omega^{(2)}$ , denoted by  $\mathcal{S}$ , is imperfect and geometrically characterized by the zero level-set of a function  $\phi: \mathbb{R}^3 \rightarrow \mathbb{R}$ :  $\mathcal{S} = \{x \in \mathbb{R}^3 \mid \phi(x) = 0\}$ . Assuming that  $\phi$  is continuously differentiable and its gradient  $\nabla\phi(x) \neq \mathbf{0}$  for all  $x \in \mathcal{S}$ , the unit normal vector field  $n(x)$  defined on  $\mathcal{S}$  and directed from  $\Omega^{(2)}$  toward  $\Omega^{(1)}$  is calculated by

$$n_i(x) = \frac{\nabla_i \phi(x)}{\|\nabla\phi(x)\|}, \quad (1)$$

As one of the significant advantages in XFEM-framed modelling and simulation, meshes are not needed to conform to the geometry of discontinuities. Usually, we first generate a regular mesh and then introduce therein the discontinuity via its level set function. Four types of elements may arise in this process, as those shown in Figure 2.

The key step in numerical modelling by XFEM consists in applying appropriate functions to describe the discontinuity of physical field by means of superimposing one or several enrichments to the conventional continuous interpolation, such that [2]

$$\mathbf{u}(\mathbf{x}) = \sum_{i=1}^{n_r} N_i(\mathbf{x})\mathbf{a}_i + \sum_{r=1}^{m_r} N_r(\mathbf{x})\psi_r(\mathbf{x})\mathbf{b}_r. \quad (2)$$

for an elasticity problem. Above,  $N_i(\mathbf{x})$  are the shape functions for a standard finite element. The functions  $\psi_r(\mathbf{x})$ , known as *enrichment functions*, influence significantly computational convergence and computational accuracy especially in the zones close to discontinuities.

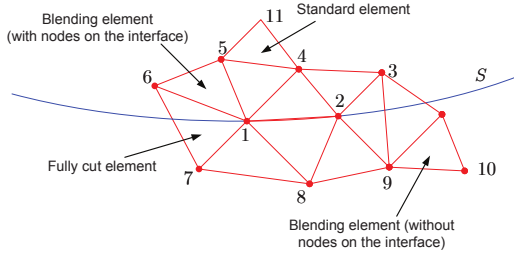


Figure 2: Four probable types of elements generated by the interface

### 3 Interface models and enrichment functions

In this part, we discuss two widely-used imperfect interface models and their modelling by XFEM.

#### 3.1 Spring-layer imperfect interfaces

Among all the models describing imperfect interfaces, the spring-layer interface model is probably the simplest one and also the most widely used one. According to this model, the displacement vector  $\mathbf{u}(\mathbf{x})$  is discontinuous across an interface while the traction vector  $\mathbf{t}(\mathbf{x}) = \boldsymbol{\sigma} \cdot \mathbf{n}$  is continuous across the same interface and proportional to the displacement vector jump

$$\llbracket \mathbf{u} \rrbracket \neq 0, \quad \llbracket \mathbf{t} \rrbracket = 0, \quad \mathbf{t} = \mathbf{K} \cdot \llbracket \mathbf{u} \rrbracket \quad (3)$$

where the second order tensor  $\mathbf{K}$  denotes the local interface stiffness. The weak form of the problem reads [4]

$$\int_{\Omega} \boldsymbol{\sigma}(\mathbf{u}) : \boldsymbol{\varepsilon}(\delta \mathbf{u}) d\Omega + \int_S \mathbf{t} \cdot \llbracket \mathbf{u} \rrbracket dS = \int_{\partial \Omega_r} \bar{\mathbf{f}} \cdot \delta \mathbf{u} dS \quad (4)$$

To describe the strong discontinuity across the interface, we propose the following enrichment function

$$\psi_r(\mathbf{x}) = \frac{1}{2} \text{sign}(\tilde{\phi}_{\mathbf{x}}) [1 - \text{sign}(\tilde{\phi}_{\mathbf{x}}) \text{sign}(\phi_r)] \quad (5)$$

where  $\tilde{\phi}_{\mathbf{x}} = \sum_{i=1}^n N_i(\mathbf{x})\phi_i$  and  $\phi_r$  is the value of the level set at node  $\mathbf{x}^r$ . It follows the displacement jump

$$\llbracket \mathbf{u} \rrbracket(\mathbf{x}) = \sum_{r=1}^{m_r} N_r(\mathbf{x})\mathbf{b}_r. \quad (6)$$

The function (5) possesses the salient features: i) it is node-dependent; ii) it contains three parts where the coefficient 1/2 allows no factor to be involved in (6), the first  $\text{sign}(\tilde{\phi}_{\mathbf{x}})$  provides the required discontinuity across the interface, and the third term  $[1 - \text{sign}(\tilde{\phi}_{\mathbf{x}}) \text{sign}(\phi_r)]$  describes the relative position of integration point  $\mathbf{x}$  and node  $\mathbf{x}^r$ ; iii) it allows removing numerical issues of some blending elements [4].

### 3.2 Coherent imperfect interfaces

The coherent imperfect interface model is appropriate for modelling the interface effect in nanomaterials and nanostructures. This model stipulates that the displacement vector is continuous across an interface whereas the stress vector suffers a jump across the same interface, which must comply with the Young-Laplace equation

$$[[\mathbf{u}]] = 0, \quad [[\mathbf{t}]] \neq 0, \quad \mathbf{div}_s(\boldsymbol{\sigma}_s) = -[[\mathbf{t}]] \quad (7)$$

The weak formulation corresponding to this model takes the form [3]

$$\int_{\Omega} \boldsymbol{\sigma}(\mathbf{u}) : \boldsymbol{\varepsilon}(\delta \mathbf{u}) d\Omega - \int_S \mathbf{div}_s(\boldsymbol{\sigma}_s(\mathbf{u})) \cdot \delta \mathbf{u} dS = \int_{\partial\Omega_e} \bar{\mathbf{t}} \cdot \delta \mathbf{u} dS \quad (8)$$

We propose the following enrichment function for coherent imperfect interfaces:

$$\psi_r(\mathbf{x}) = \frac{1}{2} \tilde{\Phi}_{\mathbf{x}} [1 - \text{sign}(\tilde{\Phi}_{\mathbf{x}}) \text{sign}(\phi_r)] \quad (9)$$

According to the level-set method, the term  $\tilde{\Phi}_{\mathbf{x}}$ , which replaces the first  $\text{sign}(\tilde{\Phi}_{\mathbf{x}})$  of (5), allows guaranteeing the continuity in displacement. Again the issues of blending elements can be removed automatically. Note that when one of element edges in 2D case or one of element sides in 3D case locates on the interface, the function  $\psi(\mathbf{x}) = \sum_{i=1}^n N_i(\mathbf{x}) |\phi_i| - |\sum_{i=1}^n N_i(\mathbf{x}) \phi_i|$ , which were proposed by Moës *et al.* [7] for perfect interface problem and followed in [3] for coherent interface problem, takes zero for all integration points inside such elements and therefore fails in describing the discontinuity of traction across the interface segment  $\mathcal{S}_{12}$  (shown in Figure 2) shared as one common side by the triangular linear elements  $\Omega_{e124}$  and  $\Omega_{e128}$ . In this sense, the proposed function (9) can remedy the above shortcoming.

### 3.3 Unified formulation of enrichment functions

Above, enrichment functions for spring-layer interfaces and coherent interfaces are proposed separately. A linear combination of the two specific functions (5) and (9) leads to a unified formulation

$$\psi_r(\mathbf{x}) = \frac{1}{2} [\xi_1 \tilde{\Phi}_{\mathbf{x}} + \xi_2 \text{sign}(\tilde{\Phi}_{\mathbf{x}})] [1 - \text{sign}(\tilde{\Phi}_{\mathbf{x}}) \text{sign}(\phi_r)] \quad (10)$$

which involves two coefficients  $\xi_1$  and  $\xi_2$  for which we propose the following material-dependent forms

$$\xi_1 = \frac{\min\{\mathcal{M}_0, \mathcal{M}_1, \mathcal{M}_2\}}{\min\{\mathcal{M}_1, \mathcal{M}_2\}}, \quad \xi_2 = \frac{\max\{\mathcal{M}_1, \mathcal{M}_2\}}{\max\{\mathcal{M}_0, \mathcal{M}_1, \mathcal{M}_2\}} \quad (11)$$

in which  $\mathcal{M}_1$  and  $\mathcal{M}_2$ , scalar-valued or norms of tensorial quantities, represent the material properties of the matrix and inclusion phases, respectively, while  $\mathcal{M}_0$  characterizes that of the initial thin interphase which has been replaced by the interface. Obviously, as expected, i) when the interphase is very soft ( $\mathcal{M}_0 \ll \mathcal{M}_1$  and  $\mathcal{M}_0 \ll \mathcal{M}_2$ ),  $\xi_1 \approx 0$  and  $\xi_2 = 1$ , the function (10) reduces to (5); ii) when the interphase is very rigid ( $\mathcal{M}_0 \gg \mathcal{M}_1$  and  $\mathcal{M}_0 \gg \mathcal{M}_2$ ),  $\xi_1 = 1$  and  $\xi_2 \approx 0$ , the function (10) reduces to (9). As it is the case in mathematical derivation, the contrast between  $\mathcal{M}_1$  and  $\mathcal{M}_2$  is assumed to be comparable.

## 4 A simple numerical example

As shown in Figure 3, the composite occupying the unit square domain is composed of the matrix and a circular rigid inclusion. The contrast in shear modulus is chosen as  $\mu_2/\mu_1 = 15$ . The interface  $\mathcal{S}$  between the bulk phases is assumed to be imperfect and can be described by the spring-layer model. For numerical computation, the domain is first discretized by a regular mesh of triangular elements. The interface is then introduced into the regular mesh via the level set function

$$f(x, y) = \sqrt{x^2 + y^2} - r \quad (12)$$

The circular inclusion domain centered at (0.5, 0.5) has the radius  $r = 0.3$ . The boundary conditions are such that  $u_x(x=0) = 0$  and  $u_y(y=0) = 0$ . The structure is subjected on the side  $x = 1$  to a uniform displacement  $u_x(x=1) = 0.001$ .

The displacement field over the deformed configurations are reported in Figure 3 (left). As expected, we observe a pronounced displacement jump in the loading direction. The smoothness of the crescent displacement discontinuity shows that the enrichment function and the relevant numerical treatment allow describing the field of the imperfect interface problem quite well (otherwise, the field of displacement jump will be saw-toothed). The right one in Figure 3 shows the distributions of the normal stress along some chosen lines passing the center and inclined at different angles  $\theta$  with respect to the  $x$ -axis. We notice that the required condition on continuity of traction vector across the interface is completely satisfied, which justifies the robustness and efficiency of the proposed numerical treatments.

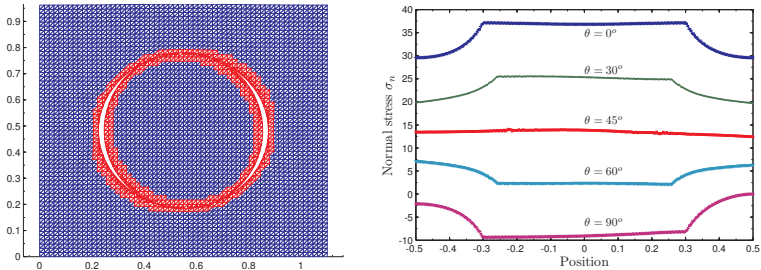


Figure 3: Displacement distributions on deformed structures (left) and distributions of the normal stresses along some lines inclined at different angles with respect to the loading direction (right)

## 5 Conclusion

The present study together with the previous works [3][4][5][6] confirm the suitability and performance of the extended finite element method in numerical modelling and simulation of discontinuous problems with typical imperfect interfaces. Enrichment functions proposed here are of unified nature and show geometric and physical consistencies. Along this line, problems with complex geometries of imperfect interfaces will be handled in future work.

## References

- [1] T. Belytschko and T. Black, *Elastic crack growth in finite elements with minimal remeshing*. International Journal for Numerical Methods in Engineering, 45: 601-620, 1999
- [2] N. Moës, J. Dolbow and T. Belytschko, *A Finite Element Method for Crack Growth without Remeshing*, International Journal for Numerical Methods in Engineering, 46 (1): 131-150, 1999
- [3] J. Yvonnet, H. Le Quang, QC. He, *An XFEM/level set approach to modelling surface/interface effects and to computing the size-dependent effective properties of nanocomposites*. Computational Mechanics, 42: 119-131, 2008
- [4] QZ. Zhu, ST. Gu, J. Yvonnet, JF. Shao, QC. He, *Three-dimensional numerical modelling by XFEM of spring-layer imperfect curved interfaces with application to linearly elastic composite materials*. International Journal for Numerical Methods in Engineering, DOI: 10.1002/nme.3175, 2011
- [5] J. Yvonnet, QC. He, C. Toulemonde, *Numerical modelling of the effective conductivities of composites with arbitrarily shaped inclusions and highly conducting interface*, Composites Science and Technology, 68: 2828-2825, 2008
- [6] J. Yvonnet, QC. He, QZ. Zhu, JF. Shao, *A general and efficient computational procedure for modelling the Kapitza thermal resistance based on XFEM*, Computational Materials Science, 50: 1220-1224, 2011
- [7] N. Moës, N. Cloirec, P. Cartraud, JF. Remacle, *A computational approach to handle complex microstructure geometries*. Comput Methods Appl Mech Eng, 192: 3163-3177, 2003